Fusion Engineering and Design 197 (2023) 114037

Contents lists available at ScienceDirect

Fusion Engineering and Design

journal homepage: www.elsevier.com/locate/fusengdes

Conceptual design of CVD diamond tomography systems for fusion devices

S. Cesaroni [a,b,*], F. Bombarda [b], S. Bollanti [b], C. Cianfarani [b], G. Claps [b], F. Cordella [b], F. Flora [b], M. Marinelli [a], L. Mezi [b], E. Milani [a], D. Murra [b], D. Pacella [b], S. Palomba [a], C. Verona [a], G. Verona-Rinati [a]

[a] "Tor Vergata" University of Rome, Industrial Engineering Department, Rome, Italy
[b] ENEA, Fusion and Nuclear Safety Department, Frascati (Rome), Italy

ARTICLE INFO

Keywords:
CVD diamond
Diamond detector
Tomography system
Soft-X ray
UV

ABSTRACT

In previous studies, excellent results have been achieved by installing Soft X-ray and UV diamond photodetectors at JET and FTU, suggesting the great potential of such devices for fusion plasma diagnostics. The main limitation in applying thin CVD diamond detectors to plasma tomography systems was the failure to detect photons with energy higher than 3 keV. In this work, we present the investigation of the detection capabilities of two additional detector layouts: the LAT diamond detector prototype, optimized for photons of energy higher than 10 keV, and the IEC diamond detector, optimized for monitoring fast events in the lower energy range. Tests have been conducted at the NIXT laboratory and with the DPP source, two ENEA Frascati Research centre facilities. The results achieved allow the design of a diamond-based tomography system for the future DTT fusion device that includes all three CVD diamond configurations for an efficient detection of radiation emitted from the hot core all the way down to the edge, as well as of the fastest phenomena associated with pellet injection and ELMs.

1. Introduction

The development of fusion as safe and reliable energy source through magnetically confined plasmas requires the plasma exhaust issue to be solved. The Divertor Tokamak Test (DTT) [1], under construction at the ENEA Frascati Research Center, will explore both conventional and alternative divertors, a key component to proceed with the design of the Demonstration Power Plant (DEMO). In order to achieve its mission, DTT has to be equipped with diagnostic tools that can qualify the particle and heat fluxes through the plasma edge and control the integrity of the plasma-facing components as well as the quality of the core plasma performance. Soft X-ray tomography is a typical diagnostic for detecting impurity accumulation and MHD activity in the hot plasma core, such as sawtooth activity or fast particles induced instabilities. However, it can also be extended to cover a wider area of the cross-section by means of detectors sensitive to UV radiation as well.

Soft X-ray and UV detectors based upon single crystal Chemical Vapor Deposition (CVD) grown diamonds were already successfully tested at JET [2] and FTU [3,4], showing higher radiation hardness and faster response compared to conventional Si diodes. In those studies, the main limitation in using such detectors for plasma tomography was the inability to detect photons with energy higher than 3 keV. Therefore, an optimization program was established to determine the most versatile and helpful set of detectors to fulfill the diagnostic requirements and cover both core and edge plasma phenomena in high-performance fusion devices. Within this framework, we present an investigation of the response of single crystal CVD diamond detectors by testing various prototypes at different facilities available at the ENEA Frascati Research Center, as follows:

- tests of a diamond detector prototype in a novel layered configuration for lateral irradiation (LAT) with one of the X-ray sources available at the New Imaging X-ray Technique (NIXT) laboratory (described in Section 2) for high energy photon detection.
- tests of diamond detectors in the planar interdigitate electrode configuration (IEC) at the Discharge Produce Plasma (DPP) EUV source [5] (described in Section 3) for fast event detection.

All the tested prototypes have been developed at the Industrial Engineering Department of the University of Rome "Tor Vergata", where the CVD diamond growth technique is well-established for high-purity layers of thickness up to 50 μm, and many diamond-based detectors have been successfully manufactured in the last 15-years [6]. The devices exhibited low leakage currents, high signal-to-noise ratios, and fast

* Corresponding author.
E-mail addresses: silvia.cesaroni@uniroma2.it, silvia.cesaroni@enea.it (S. Cesaroni).

https://doi.org/10.1016/j.fusengdes.2023.114037
Received 30 October 2022; Received in revised form 5 August 2023; Accepted 18 October 2023
Available online 21 October 2023

time responses (below 1 ns). A tomographic system based on this type of diamond detectors is proposed for the DTT project, as explained in Section 4. A comprehensive discussion of the results achieved, and a view of future developments are reported in Section 5.

2. Tests at NIXT laboratory with X-ray sources

2.1. The LAT diamond detector prototype

The improvement of diamond detector's ability to efficiently detect Soft X photons with energy $E>2$–3 keV requires a thickness of the active layer that cannot be obtained through standard diamond growth techniques. For this reason, a novel detector configuration which allows the lateral irradiation of the diamond layer has been studied. To increase the detection efficiency of the device, the area exposed to incident photons has been expanded by coupling two CVD diamonds grown on a 3×3 mm^2 High-Pressure High-Temperature (HPHT) diamond substrate in a p-type/intrinsic layered structure. They were assembled one above the other and electrically connected by the metal contact deposited upon each single crystal diamond intrinsic layer, as shown in Fig. 1. It is important to note that the application of the metal contact upon the diamond layer was performed using a thermal evaporation system and foresaw the usage of a mask, forbidding the metal deposition up to the layer edge. For this reason, incident photons must have sufficient energy to cross a diamond dead layer before being detected.

The diamonds assembly was mounted on a vetronite printed circuit board (PCB). The electrical connection has been realized using microwelds. This kind of electrical contacts layout allows using the prototype as Schottky photodiodes without needing external bias. The signals were recorded using a FEMTO trans-impedance amplifier (gain of 10^8V/A) and an oscilloscope. The detector assembly has been incorporated in an epoxy resin matrix for insulation and ease of handling. The side of the device exposed to irradiation has been lapped in order to reduce the surface roughness and minimize the diamond dead layer met by incident photons.

Studies performed in the past experimentally confirmed the analytical estimates of the responsivity for thin-layered detectors [7]; an approximated calculation of the responsivity curves at different energies of the incident radiation performed for different thicknesses of the active diamond layer is shown in Fig. 2.

Compared to the previous design of diamond photodetectors, for which the detection capability was limited to energies of a few keV, the innovative layout of the device allows photons to be absorbed along its full 3 mm lateral extension, enabling the detection of X-rays with energy

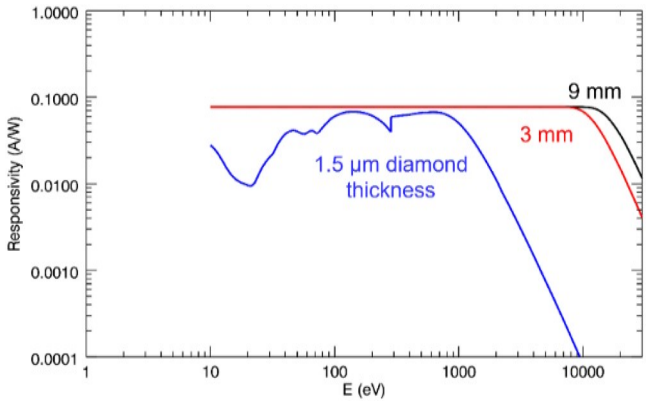

Fig. 2. Calculation of the approximated detector's responsivity to photons of different energies for various diamond thicknesses: 1.5 µm in blue, 3 mm in red, and 9 mm in black.

$E \geq 10$ keV, albeit with a strongly non-linear decreasing efficiency above this value. Furthermore, the calculation shows that there is no significant advantage in increasing the detection thickness above few millimeters due to the physical characteristics of the diamond crystal. Given the manufacturing issues explained above, also the low energy photons are being cut-off, therefore we can consider this configuration as a high-pass filter.

2.2. The X-rays source

The NIXT Laboratory at the ENEA Frascati Research Center provides X-ray tubes, sources, filters, and calibrated detectors. It is fully shielded up to 120 keV and equipped for gas and solid-state detectors and spectrometers. The experimental configurations can be simulated with absolute spectra distribution and the devices can be remotely controlled.

The X-ray source utilized in our tests is the Jupiter 5000 series tube produced by Oxford Instruments, cooled by forced air. The target material of the anode, where the X-rays production takes place, is Tungsten (W, $Z = 74$). The supply voltage and the beam current can vary up to 50 kV and 1000 µA respectively: the first parameter is directly related to the maximum energy of the emitted X-photons, while the source strength varies linearly with the beam current. The spectra of the source with 100 µA of beam current and different supply voltage values (Fig. 3a) have been recorded using a 1 mm thick CdTe detector, which exhibits nearly a 100 % efficiency in the energy range 7÷60 keV.

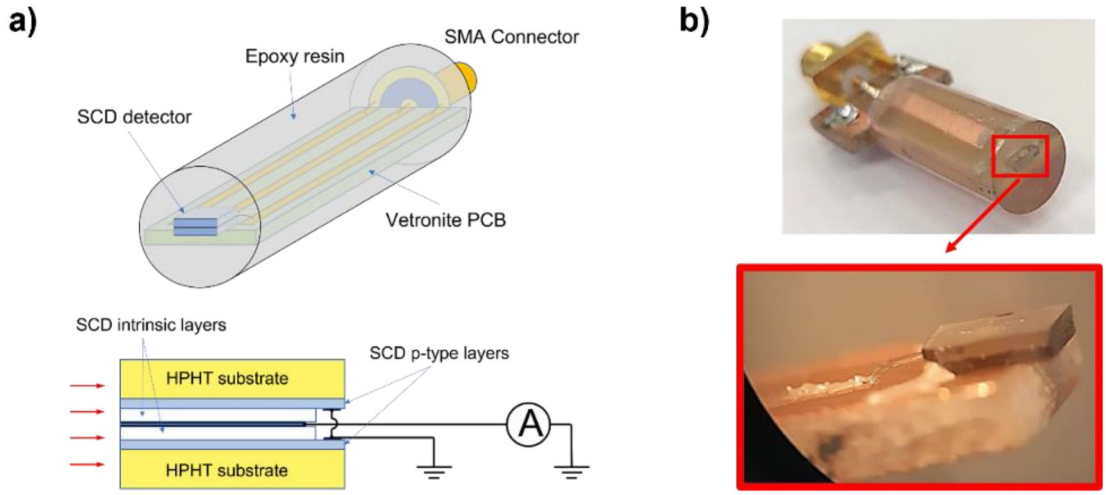

Fig. 1. The novel diamond detector LAT prototype: a) a scheme of the layout and the simplified electrical diagram; b) a picture of the device with a magnification of the diamonds assembly under the microscope.

With the W anode, the X-ray emission below 10 kV is very weak, and, at 5 kV, it was not possible to measure any signal. This low energy detection limit, however, needs further investigation because it could be caused by the relatively noisy environment of the measurement set-up and possible edge effects of the LAT detector, both of which can be improved upon.

In Fig. 3b, a comparison between the two detectors (i.e. diamond prototype and CdTe detector) is shown: the CdTe detector performs better at higher photon energies, while the diamond becomes less sensitive as a result of the decrease of the responsivity curve (see Fig. 2).

2.3. Results

The diamond prototype has been tested under X-irradiation up to 50keV. However, at HV_{source}=5kV the diamond response was below the noise level, even at the highest source current. Therefore, those data have been disregarded. We consider this to be a problem related to the quality of the diamond-exposed surfaces and of the metal contacts, which were hand lapped and likely not to be sufficiently conductive to provide the expected response.

Since low energy photons give the main contribution to the diamond response, the source emission spectra have been computed taking into account the analytical fitting of the responsivity curve in the range 10÷50keV, as shown in Fig. 4a. In Fig. 4b, the ratio between the diamond prototype response and the integral of the computed spectra of Fig. 4a is shown as a function of the source supply voltage: the diamond detector resulted to always maintain the same proportionality with the CdTe detector counts for different source strength.

Diamond prototype response (I_{diam}) always resulted in being proportional to the source emission spectra, growing linearly with the increasing source strength (i.e. the beam current, I_{source}), as shown in Fig. 5a and 5b for a different supply voltage of the source.

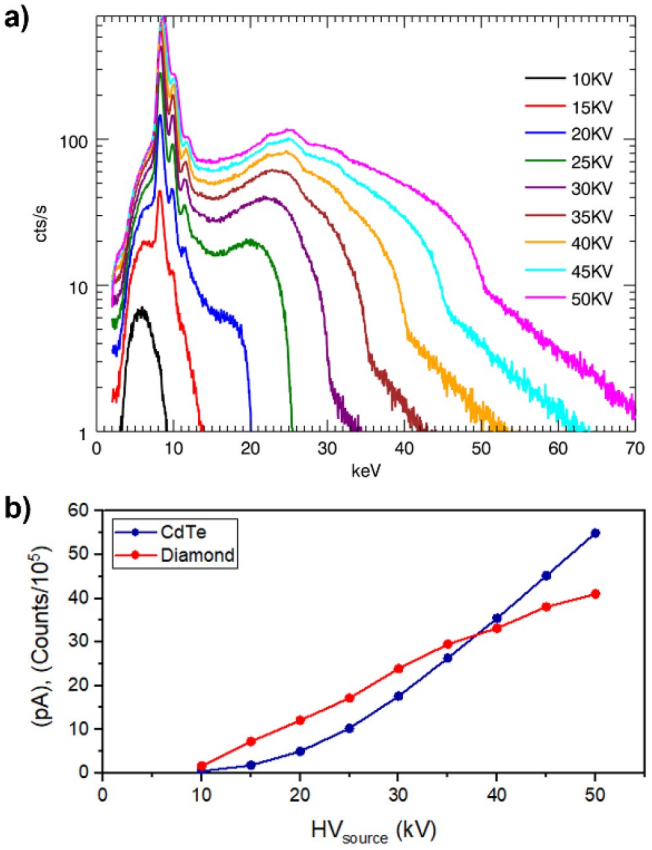

Fig. 3. a) X-ray emission of the source operated at 100 μA of beam current and supply voltage varying from 10 kV up to 50 kV; b) response comparison between the CdTe detector and diamond prototype.

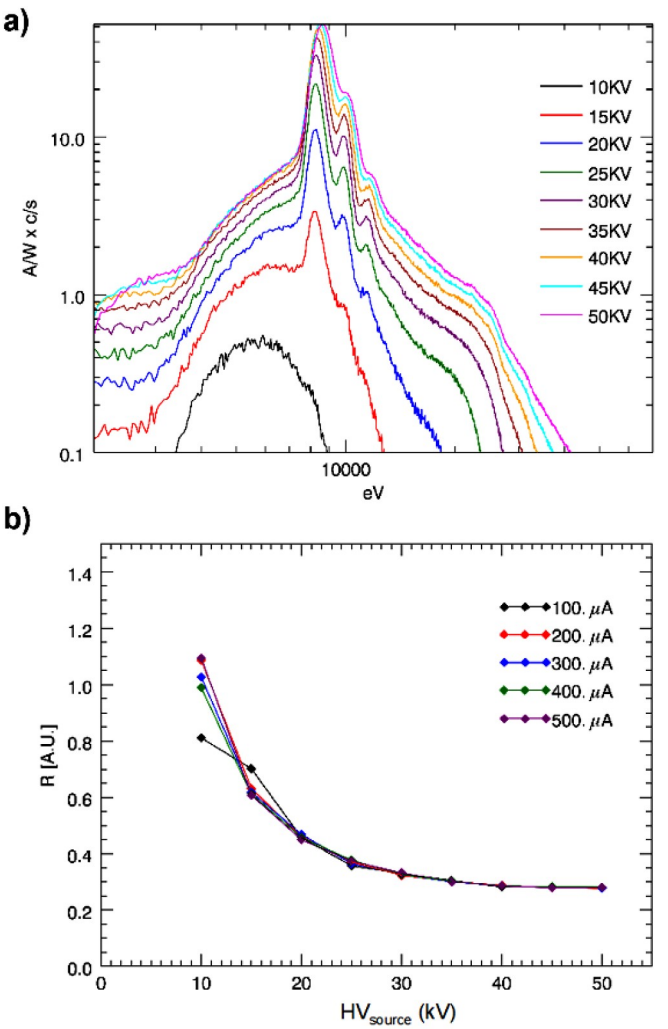

Fig. 4. a) Source emission spectra calculated taking into account the diamond prototype responsivity; b) diamond prototype response divided by the integral of the source spectra shown in a) as a function of the source HV for different source strength.

Calibrated Aluminum filters have been employed to cut the spectrum's lower part and better study the diamond prototype response. The transmission curves of the Al filters used during the tests are reported in Fig. 5c. The results confirmed that the most significant contribution to the diamond prototype signal is given by low-energy photons, as shown by the amplitude of the filtered signals recorded at 45kV source supply voltage and reported in Fig. 5d. The comparison with the signal recorded on the full source spectrum at the same conditions demonstrates that the 100μm Al filter, absorbing 50 % of 10keV photons, causes a reduction of the detector signal of more than half concerning the no-filter condition.

3. Tests at the DPP EUV source

3.1. The IEC diamond detector

The IEC diamond detector consists of a CVD diamond intrinsic layer homoepitaxially grown on a 3×3 mm^2 HPHT diamond substrate, with two Cr interdigitated comb-shaped electrodes patterned by standard photolithography on the intrinsic diamond surface, as shown in Fig. 6. The Cr electrodes are about 100 nm thick and their structure, operating in a planar configuration, acts as a two terminal metal-diamond-metal

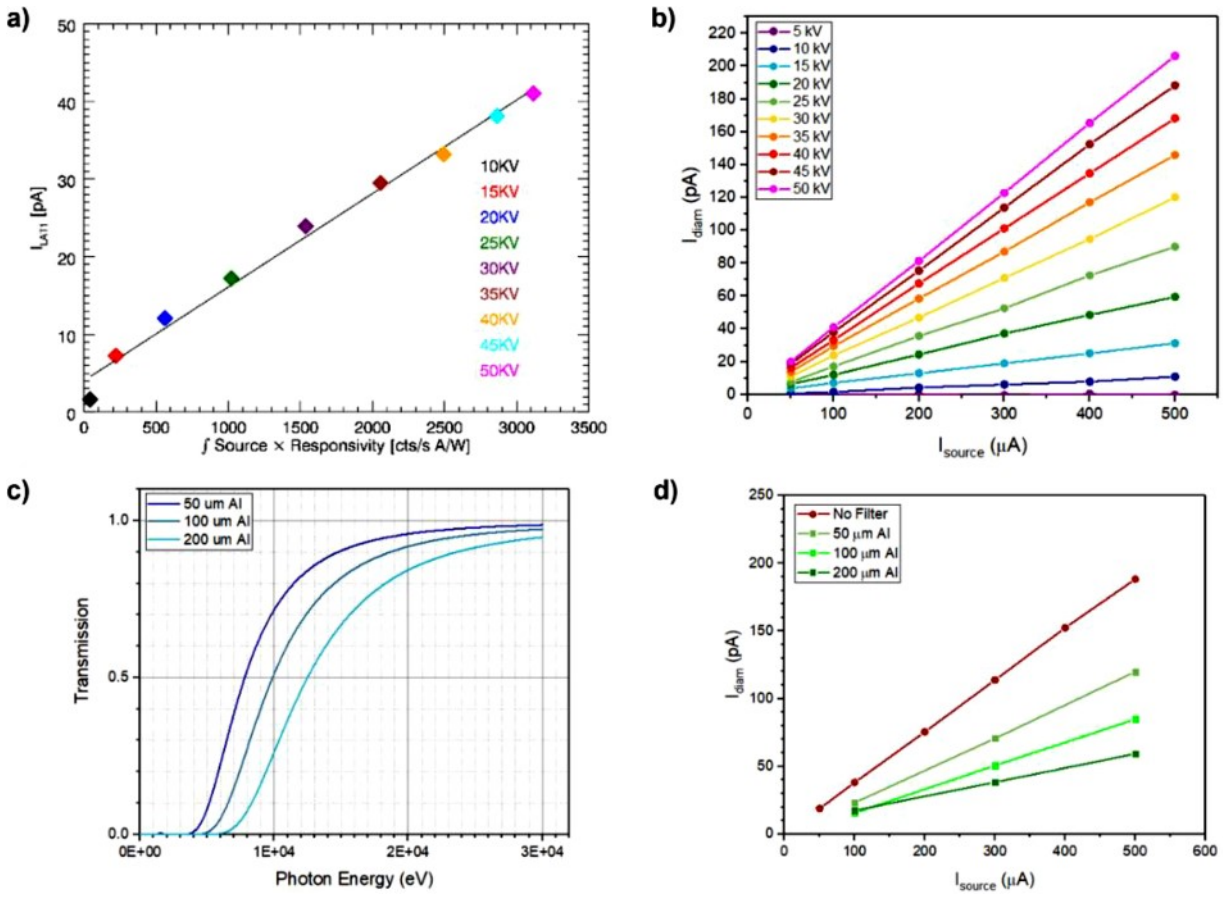

Fig. 5. a) Diamond prototype response to computed spectra at 100 μA of beam current; b) diamond detector response to increasing source strength at different source supply voltage; c) the transmission coefficient of Al filters calculated for 50, 100, 200 μm thickness; d) comparison between the diamond prototype signal with and without the Al filters in front of the X-rays source.

(MDM).

The detector was mounted on a holder equipped with a bias tee and placed inside the facility's vacuum at a distance of about 43cm from the EUV source.

Detectors listed in Table 1 have been produced and tested, each characterized by the different spacing between two electrodes and the nominal width of the fingers. In order to establish an electric field able to collect the charges generated inside the diamond layer by the impinging EUV radiation, a biasing voltage of −80 V was applied to each detector.

3.2. The EUV source

The DPP EUV source operates at the ENEA Frascati Research Center [8]. The facility is optimized to emit EUV pulses with photons of energies E=69÷124eV. Typically, low pressure Xe gas (0.5÷1.5 mbar) is used, which exhibits the main emission EUV band in the wavelength range λ= 10÷18 nm. The plasma formation is achieved with two consecutive electric discharges: the first at a lower current (~30 A) and more extended in time (~20 μs) for the gas pre-ionization, and the main fast discharge with high current (~12÷13 kA peak, ~240 ns half-period).

In Table 2, the main DPP source parameters are summarized.

Among the diagnostics of the facility, a silicon PIN-diode EUV radiation detector placed inside the vacuum chamber at a 50 cm distance from the source is used as a reference for the signal recorded by the diamond detector. The PIN-diode and the diamond detector signals are recorded using a high-frequency oscilloscope featured by a 50 Ω input impedance. In order to properly select the source emission wavelength region, Zr filters have been applied in front of both detectors.

3.3. Results

The three IEC diamond detectors have been tested under EUV irradiation and compared to the signal recorded with the PIN-diode. Their response was very similar because the diamond volume sensitive to photons is confined to a small region around the electrodes and does not change significantly in the three considered layouts. The comparison between the IEC diamond detector and the PIN-diode signals is reported in Fig. 7. The diamond detector exhibited a faster response, resulting in a smaller rise-time of the peak associated with the EUV photons emission and a more detailed time evolution of the plasma discharge, allowing a better characterization of the source.

This result, to some extent already established in previous tests of IEC detectors in different experimental conditions [9,10], provides a validation for their possible use to detect the intense, but low energy radiation emitted, for example, by ablating D pellets injected into the plasma, and by ELMs, fast edge instabilities that are one of the main concerns for the survivability of the plasma facing components in future tokamaks. An example of such application from JET is reported in [11], although with lower time resolution.

4. Diamond-based tomography system for future fusion devices

The experience gained on JET and FTU, with the additional results reported in the previous sections, have confirmed the validity of the proposal of a full tomographic system based on diamond photodiodes for the DTT machine presently under construction at Frascati, and possibly for other devices due to operate at very demanding plasma parameters and high neutron fluxes, where the survivability of conventional Si/Ge

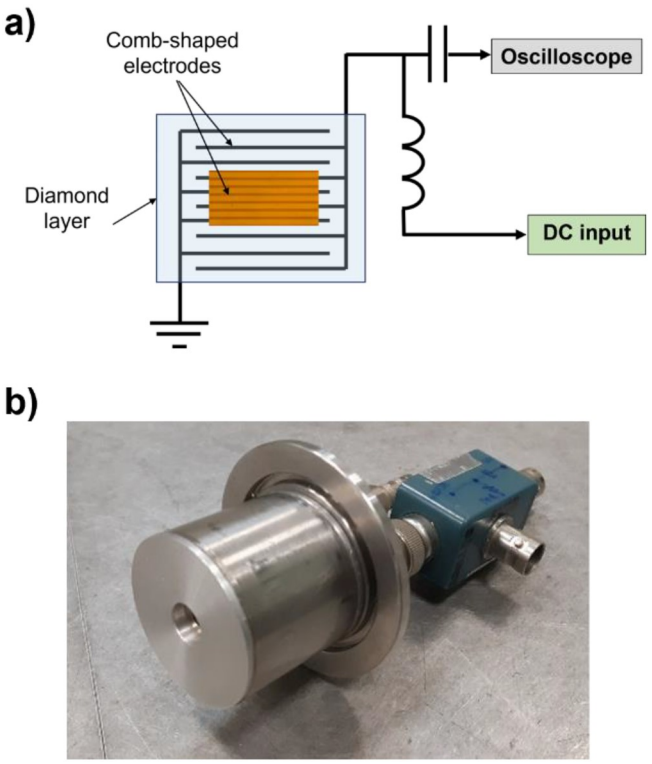

Fig. 6. The IEC diamond detector layout: a) the simplified electrical diagram with an inset of the contacts seen under the microscope and b) a picture of the device.

Table 1
List of the IEC diamond detectors tested at the DPP EUV source.

	Electrode finger [μm]	Gap [μm]
IEC #1	5	5
IEC #2	10	10
IEC #3	5	20

Table 2
Main characteristics of the DPP EUV source.

Gas filling	Xenon (5 ÷ 15 sccm)
EUV emission wavelength	$\lambda = 10 \div 18$ nm
Energy per pulse	~ 30 mJ / pulse / sr
First peak time length	~ 100 ns
Repetition rate	10 ÷ 20 Hz
Source diameter	~ 300 μm
Source emission cone	0.96 sr
Discharge current half-period	240 ns

detectors would be much shorter. In particular, the CVD diamonds radiation hardness was assessed in [12] for 500 μm layer thickness, and it is expected to be much better for thinner photodiodes. We demonstrated that CVD diamonds in different configurations could be employed to cover the entire plasma cross-section, from the hot core, with temperatures over 10 keV, to the plasma edge, thanks to the diamond sensitivity reaching down to 5.5 eV, without being affected by the visible radiation. This opens up opportunities for improved diagnostics capabilities, but the actual design has to be developed.

The tomography system for DTT foresees the possibility of installing arrays of CVD diamonds in four of the five poloidal ports at one toroidal location. A tentative geometry is shown in Fig. 8, where 96 LoS should provide sufficient chords for good reconstructions (presently under study). In contrast, a few more diodes covering the SOL and the pedestal

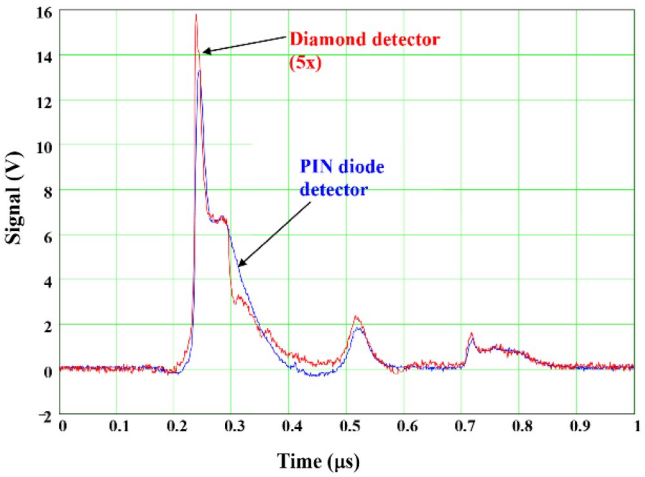

Fig. 7. Comparison between the IEC diamond detector and the PIN-diode responses during tests at the DPP EUV source.

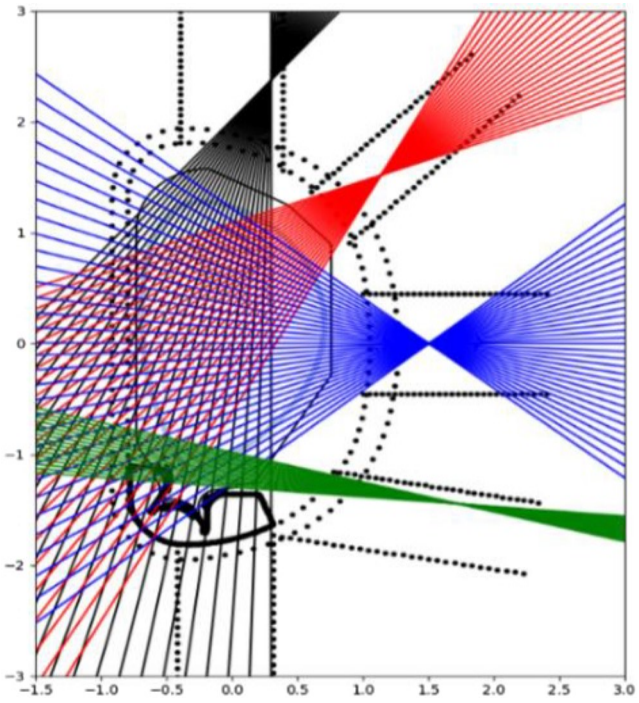

Fig. 8. Tentative layout of the DTT tomography system with 96 LoS covering the poloidal cross-section from four ports at one toroidal location.

regions with a toroidal view can provide valuable information about detachment, and other fast phenomena, such as ELMs and pellet ablations.

The detector arrays layout for DTT tomography system is still under assessment and was made possible thanks to the extremely small size of the CVD diamond detectors. The lack of the need for Be windows and cooling system (required for Si/Ge diodes), and the larger spectral region covered by the innovative diamond detectors make their use very affordable compared to conventional solutions.

For such a large number of detectors, a suitable multichannel, low-noise current preamplifier module is under development by CAEN, with variable trans-impedance gain and 500 kHz bandwidth.

5. Discussion and conclusion

A novel diamond detector configuration was developed and tested at the NIXT laboratory of ENEA Frascati with X-rays in the energy range of 5÷50 keV. The irradiation tests produced good results concerning the diamond prototype response and confirmed the previously calculated diamond sensitivity to photons of different energy. Despite the diamond prototype signal mainly being caused by low energy photons, the detector response at higher energy was neatly recordable. In fact, the manufacturing complication of the double layer in the LAT configuration can be avoided using a single layer of equivalent thickness. Other tests performed at the DPP EUV source investigated the IEC diamond detector response to photons of energy up to 124 eV, confirming the fast response capability of the device. This feature constitutes an advantage that can be used in fusion plasma diagnostics to detect very fast phenomena occurring at the plasma edge, such as ELMs.

Further results will be achieved by an array of five detectors with different line-of-sights presently being installed on the Protosphera device [13], which will also enable testing a multichannel pre-amplifier under development expressly for application to large diode arrays. To fulfill the requirements of the diamond-based tomographic system proposed for DTT, an optimization of the detector layout is still needed in order to be able to identify both core and plasma edge phenomena. Further tests using calibrated monochromatic sources at a synchrotron facility are planned in order to deeply investigate the diamond detector responsivity to photons with energies both higher and lower than those considered in the present study.

Declaration of Competing Interest

The authors declare that they have no known competing financial interests or personal relationships that could have appeared to influence the work reported in this paper.

Data availability

Data will be made available on request.

Acknowledgments

This work was supported in part by the DTT task 2022-DIA-DIC/DOC-1. The authors also wish to thank Dr. M. Iafrati for making available his codes and provide valuable insight on the definition of the tomographic inversion problem.

References

[1] Divertor Tokamak Test Facility, Interim Design Report, ENEA press, 2019. ISBN: 978-88-8286-378-4.
[2] M. Angelone, et al., Nucl. Instrum. Methods A 623 (2010) 726, https://doi.org/10.1016/j.nima.2010.04.021.
[3] F. Bombarda, et al., Nucl. Fusion 61 (2021), https://doi.org/10.1088/1741-4326/ac233a.
[4] S. Cesaroni, et al., Fusion Eng. Des. 166 (2021), 112323, https://doi.org/10.1016/j.fusengdes.2021.112323.
[5] L. Mezi, et al., Nuovo Cimento 45 C (2022), https://doi.org/10.1393/ncc/i2022-22088-5.
[6] S. Almaviva, et al., J. Appl. Phys. 103 (2008), 054501, https://doi.org/10.1063/1.2838208.
[7] I. Ciancaglioni, et al., J. Appl. Phys. 110 (2011), 054513, https://doi.org/10.1063/1.3633219.
[8] L. Mezi, F. Flora, ENEA Technical Report, 2012, 15/2012.
[9] M. Marinelli, et al., Appl. Surf. Sci. 272 (2013) 104, https://doi.org/10.1016/j.apsusc.2012.05.142.
[10] R. De Angelis, et al., JINST 11 (2016), https://doi.org/10.1088/1748-0221/11/12/C12048. C12048.
[11] R. Rossi, et al., Appl. Sci. 12 (2022) 3681, https://doi.org/10.3390/app12073681.
[12] M. Pillon, et al., J. Appl. Phys. 104 (2008), 054513, https://doi.org/10.1063/1.2973668.
[13] F. Alladio, et al., Nucl. Fus. 46 (2006), https://doi.org/10.1088/0029-5515/46/8/S07. S613.